Energy & Environmental Science

Cite this: *Energy Environ. Sci.*, 2012, **5**, 9833

www.rsc.org/ees

PAPER

Activated carbon monoliths for gas storage at room temperature

J. P. Marco-Lozar,[a] M. Kunowsky,[a] F. Suárez-García,[a] J. D. Carruthers[b] and A. Linares-Solano*[a]

Received 5th July 2012, Accepted 1st October 2012
DOI: 10.1039/c2ee22769j

Porous materials are interesting candidates for gas storage in different applications. The present study analyses at room temperature the high pressure storage of H_2, CH_4 and CO_2 in a number of porous carbons (eight monoliths and two powdered activated carbons). The samples cover a wide range of porosities and densities (monoliths having high porosity with moderate density or moderate porosity with high density) with the aim to discuss the relative importance that the sample surface area has on the volumetric storage capacity, in relation to the importance of the density of the material. Our results show that the gravimetric storage capacities of the three studied gases are controlled by the textural properties of the adsorbent, whereas the volumetric storage capacities are mainly controlled by the adsorbent density. High volumetric excess adsorption capacity values (for example, H_2: 10 g l^{-1}; CH_4: 110 g l^{-1} and CO_2: 440 g l^{-1}) correspond to monoliths having high densities, despite their moderately developed porosities. This paper also compares these results with those obtained similarly (same gases and same experimental conditions) using the highest known surface area material (MOF-210). In summary, our volumetric results, obtained with commercially available ATMI monoliths and their CO_2 activation, are, to the best of our knowledge, amongst the highest that have been reported; higher than the high surface area samples of the M3M monolith prepared from Maxsorb (S_{BET}: 2610 m^2 g^{-1}) or MOF-210 (S_{BET}: 6240 m^2 g^{-1}). Although a variety of MOFs have been reported to exceed our results, oftentimes these values are overestimated due to the fact that the volumetric capacity of MOFs was calculated using crystal density rather than experimentally measured density.

1. Introduction

In recent decades, there has been an increasing interest to develop gas storage systems for different fields such as energy applications (*e.g.*, on-board storage of H_2 and CH_4 for transportation technologies) or for environmental purposes (*e.g.*, carbon dioxide capture due to concerns over greenhouse gas emissions, volatile organic compound (VOC) transportation, or safe transportation of very dangerous compounds).[1] One of the technologies that has been proposed for gas storage application is the use of porous materials having high adsorption capacities.[1–8] Thereby, the gas is accumulated in the pores of these materials due to the attractive forces that are established between

[a]*Grupo de Materiales Carbonosos y Medio Ambiente, Departamento de Química Inorgánica, Universidad de Alicante, Ap. 99, E-03080 Alicante, Spain. E-mail: linares@ua.es; Fax: +34 965 90 34 54; Tel: +34 965 90 35 45*
[b]*ATMI, Adsorbent & Gas Technology, Danbury, Connecticut 06810, USA*

Broader context

The storage of gases like hydrogen, methane, and carbon dioxide is very important for energy and environmental applications. The emission of carbon dioxide to the atmosphere increases the earth's greenhouse effect, leading to an increase of the global temperature. A possible solution is its capture and sequestration. Hydrogen and methane may substitute gasoline as fuel in transportation technologies. Their main advantage is that they can be produced from renewable energy sources like solar, wind or biomass, reducing the emission of carbon dioxide. From an application point of view, an important factor for the storage of these gases is to reduce the volume of the storage tank. A promising technology is physical adsorption on porous materials with high adsorption capacities. Thereby, the gas molecules are attracted to the highly porous structure of the material. This paper investigates the adsorption of hydrogen, methane, and carbon dioxide at room temperature and high pressures on a number of activated carbon monoliths, some of which have the highest density reported for this kind of materials. Exceptionally high volumetric excess adsorption capacity values are reached for all of the three gases, especially taking into account their realistic (measured) material bulk densities.

gas molecules and materials.[9] Several types of adsorbents are continuously being developed and tested. Among the great variety of possible porous materials, the best candidates for this application are materials with a high development of pores with suitable sizes. Thus, "classical adsorbents" like porous carbon materials – such as activated carbons (AC) or activated carbon fibers (ACF) – or zeolites and "new adsorbents," like metal organic frameworks (MOF) or covalent organic frameworks (COF), are currently the subject of research.[1–8,10–16] Independent of its nature, the adsorbent material designed for these applications should meet the following characteristics: (i) composed of light elements; (ii) high stability under working conditions; (iii) chemical inertness; and (iv) high density.

When an adsorbent has to be selected for its application in gas storage at high pressures, this selection can be done taking into account two different possibilities: (i) based on its capacity on a gravimetric basis (adsorption per gram of adsorbent), where textural properties (surface area, porosity and pore size distribution) are mainly the parameters that control the adsorption[17–19] or (ii) depending on its capacity per litre of adsorbent (on a volumetric basis; the most suitable way to express the results from a storage application point of view), in which not only the textural properties but also the density affects the gas uptake.[20–22]

It has been demonstrated that the density of the adsorbent has an important effect on the storage capacity. In practice, the adsorbent has to be confined in a given volume, and the higher the adsorbent density, the higher the amount of material which can be confined in a tank and, hence, the higher the storage capacity.[1,3,8,16]

Although some studies have highlighted the importance of the porosity and the density on the gas storage capacity,[1,3,8,16,20–24] further investigations are necessary to study such important influence of the adsorbent density on its final storage capacity. To reach, for a given adsorbent, a maximum gas storage capacity, both its adsorption capacity and its density have to be maximized.

In this paper, we analyse and evaluate in depth the influence that both parameters have on the gas storage at room temperature of hydrogen, methane and carbon dioxide. For this purpose, our study is focused on selected carbon monoliths (commercial and carefully laboratory prepared monoliths) having opposite properties: high adsorption capacities and moderate densities or having moderate adsorption capacities and high densities. Additionally, our results are compared with those similarly obtained (same gases and same experimental conditions) with the material that exhibits the highest surface area and pore volume reported to date (MOF-210).[11,25]

2. Experimental

2.1. Adsorbent materials

For this investigation two types of adsorbents with different properties were selected: (i) on the one hand, two (commercially available (BrightBlack™)) carbon monoliths (A1 and A3) provided by ATMI Co. which are generated by pyrolysis of a PVDC copolymer (A1 submitted to a higher degree of activation in nitrogen than sample A3). These samples are commercial carbon monoliths with probably the highest density values. Cylindrical monoliths with 10 mm diameter and 13 mm height were physically activated with CO_2 at different activation times (*i.e.*, 12, 24, 36 and 48 hours) in order to increase the porosity development, thereby trying to avoid the reduction of its density. (ii) On the other hand, for comparison purposes, two activated carbon monoliths (M3M and K1M) were prepared from two highly activated carbon powders by using a polymeric binder from Waterlink Sutcliffe Carbons. One of them (M3M) came from a well known commercially available high surface area activated carbon (Maxsorb 3000, from Kansai Coke & Chemicals) and the second one from an activated carbon prepared in our laboratory by chemical activation with KOH of a Spanish anthracite following the experimental process previously described.[26] The preparation conditions for these monoliths (type of binder, percentage of binder, pressing temperature and carbonization) were selected from the results previously studied by our research group.[27] For this preparation, the amount of binder added was 15 wt%. The binder/activated carbon mixtures were dried and then pressed into a cylindrical mould with 1.6 cm diameter which was heated up to 135 °C.[27] The obtained monoliths were then pyrolysed at 750 °C for 2 h in a horizontal furnace under an inert atmosphere in order to carbonise the binder.

2.2. Activation process

In order to modify the porosity of the A-series, the monolith having better porosity and density characteristics (A3; see Table 1) was submitted to a physical activation, without introducing important changes in the adsorbent density. The A3 carbon monolith was heat treated in a horizontal furnace. The furnace was first purged with a nitrogen flow of 100 ml min^{-1} for about 30 minutes. After that, the sample was heated under the nitrogen flow at a heating rate of 20 °C min^{-1}, up to the desired activation temperature of 800 °C. Once the activation temperature was reached, nitrogen flow was switched to CO_2 (100 ml min^{-1}). These conditions remained constant during the desired activation time. Afterwards, the gas flow was switched again to 100 ml min^{-1} of N_2, and the furnace was cooled down. The nomenclature used for the A3 activated monoliths includes the time of activation.

2.3. Textural characterization and densities

The porous texture characterization of all activated carbon materials was assessed by physical gas adsorption of nitrogen and CO_2 adsorption at −196 and 0 °C respectively, in an ASAP-2020

Table 1 Porosity characterization of the A-series carbon monoliths selected in the present study, deduced from the N_2 and CO_2 adsorption isotherms at −196 and 0 °C, respectively, piece densities and the activation yields for the activated carbon monoliths

Monolith	S_{BET}, $m^2\ g^{-1}$	V_{DR} (N_2), $cm^3\ g^{-1}$	V_{DR}, (CO_2), $cm^3\ g^{-1}$	Density, $g\ cm^{-3}$	Act. yield, %
A1	928	0.43	0.44	1.00	—
A3	941	0.43	0.45	1.07	—
A3-12	988	0.56	0.50	0.99	85
A3-24	1145	0.66	0.57	0.93	79
A3-36	1367	0.71	0.50	0.87	68
A3-48	1586	0.77	0.50	0.80	67

device (Micromeritics Co.). The samples were outgassed at 250 °C under vacuum for 4 hours. Apparent BET surface areas, Dubinin–Radushkevich micropore volumes, and DFT pore size distributions were calculated from nitrogen adsorption data. Narrow micropore volumes (pore sizes smaller than 0.7 nm) were calculated from CO_2 adsorption at 0 °C using the Dubinin–Radushkevich equation.[28–30] Piece densities of the samples, clearly defined due to the monolithic nature of the carbons, were measured at RT and calculated using the weight and the geometric volume of the carbon monoliths.

2.4. Gas adsorption

The adsorption of the different gases studied at room temperature (hydrogen, methane and carbon dioxide) has been measured using different equipments, depending on the required pressure.

For H_2 adsorption at room temperature and up to 200 bar, a fully automated volumetric apparatus, designed and built at the University of Alicante, was used.[19,31] About 700 mg of the sample were degassed at 150 °C during 4 hours under vacuum and the weight of the degassed sample was measured. After that, the sample was located in the sample holder, where it was degassed at 150 °C during another 4 hours in vacuum, in order to prepare the sample for the measurement. The bulk gas densities were calculated by a modified Benedict–Webb–Rubin equation of state proposed by Younglove.[32]

Excess adsorption isotherms of CH_4 and CO_2 were measured for pressures up to 30 bar in a Sartorius 4406-DMT high-pressure microbalance. In case of both gases, about 500 mg of the sample were placed in the sample holder and degassed *in situ* at 150 °C under vacuum until a constant weight was measured. The experimental results were corrected for buoyancy effects related to the displacement of gas by the sample, sample holder and pan.[33]

3. Results and discussion

3.1. Textural characterization

Table 1 contains the porous texture characterization results together with the piece densities of the pristine carbon monoliths (A1 and A3) and the CO_2-activated carbon monoliths obtained from them. From the textural results it can be seen that the pristine monoliths (A1 and A3) have a moderate porosity, but interestingly high densities (as high as around 1 g cm^{-3}). For the physically activated samples, the increase in the activation time provokes a progressive increase in adsorption capacity. As was expected, CO_2-activation leads to a reduction of the piece densities. For the maximum activation time of 48 hours, a BET value of 1586 m^2 g^{-1} and a density of 0.8 g cm^{-3} are reached. Thus, even for the highest activation time, the obtained density is still quite elevated compared with those of other carbon monoliths prepared from powdered porous carbons[20,34] and it is similar to reported values for high density carbide derived carbons (CDC) prepared from ceramic TiC plates.[21]

Fig. 1 shows the N_2 adsorption/desorption isotherms at −196 °C for the A monoliths and the corresponding CO_2 activated samples. From the shapes and type of the obtained isotherms (type I of the IUPAC classification), it can be concluded that, in general, all the samples present a marked

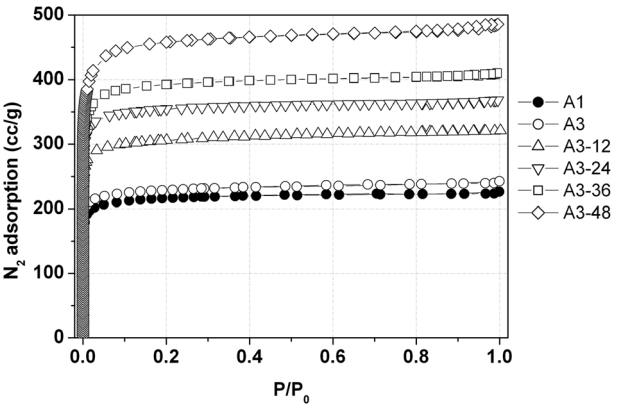

Fig. 1 N_2 adsorption/desorption isotherms at −196 °C for the pristine carbon samples (A1 and A3) and physically activated monoliths.

microporous character. Furthermore, the isotherms show a plateau reflecting a minimum presence of mesopores. The knees of the isotherms are quite close, indicating a narrow micropore size distribution. This is clearly observed in their pore size distribution, as shown in Fig. 2. Thus, pristine monolith A3 has a very narrow pore size distribution with the maximum at 0.53 nm with some small proportion extending as far as 0.7 nm. A low activation process (<24 h) causes a slight broadening of the pore size distribution and a development of some micropores between 0.7 and 1 nm. At high activation times (>24 h), the widening of the pore size distribution continues and there is a shift of the maximum peak to 0.61 nm; and wider micropores are developed with the appearance of a new peak centred at 0.85 nm for monoliths A3-36 and A3-48.

In summary, the CO_2 activation process carried out provokes a continuous increase in the adsorption capacity (Fig. 1) together with a modest widening of the micropore size distribution (Fig. 2) which is maintained below 1 nm.

Fig. 3 presents N_2 adsorption/desorption isotherms at −196 °C for the samples (M3 and K1) and their monoliths (M3M and K1M) and Table 2 summarizes their porosity characterization, deduced from N_2 (−196 °C) and CO_2 (0 °C) adsorption isotherms and piece densities of the carbon monoliths. In contrast to the A-series materials (see Table 1), the monoliths that were prepared from powdered activated carbons (M3M and

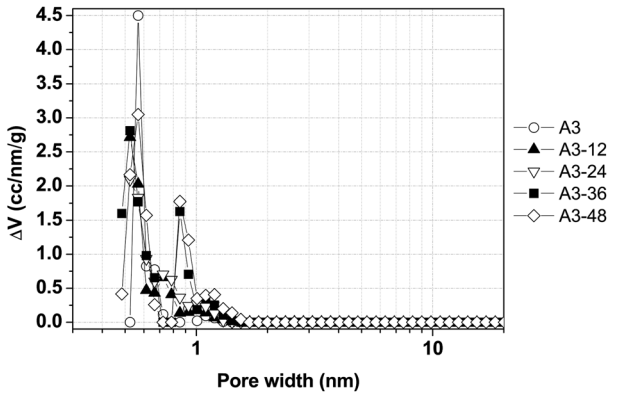

Fig. 2 DFT pore size distributions for samples A3 and its CO_2-activated monoliths.

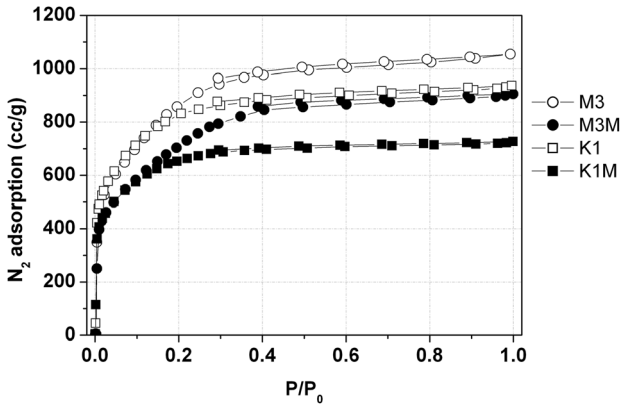

Fig. 3 N_2 adsorption/desorption isotherms at −196 °C for the samples (M3 and K1) and their monoliths (M3M and K1M).

Table 2 Porosity characterization of the activated materials M3 and K1 and their monoliths, deduced from N_2 (−196 °C) and CO_2 (0 °C) adsorption isotherms and piece densities of the carbon monoliths

Sample	S_{BET}, $m^2\ g^{-1}$	V_{DR} (N_2), $cm^3\ g^{-1}$	V_{DR} (CO_2), $cm^3\ g^{-1}$	Piece density, $g\ cm^{-3}$
M3	3180	1.31	0.70	—
K1	3120	1.25	0.72	—
M3M	2610	0.93	0.60	0.42
K1M	2320	0.91	0.59	0.50

K1M) have a considerably higher porosity, reaching BET surface areas higher than 2000 $m^2\ g^{-1}$, V_{DR} (N_2) superior to 0.9 $cm^3\ g^{-1}$, and V_{DR} (CO_2) around 0.6 $cm^3\ g^{-1}$. However they are much less compact, having half of the density in comparison with those of the monoliths derived from ATMI.

The use of a binder for the preparation of the monoliths produces a reduction in the N_2 and CO_2 adsorption capacities. However, the obtained monoliths show adsorption capacities at least two times higher than the samples of the A series.

The adsorption isotherm shapes of Fig. 3 show that M3 (and its corresponding M3M monolith) has higher adsorption capacity than K1 (and its corresponding K1M monolith) and a wider porosity (see their pore size distribution in Fig. 4). All samples have similar pore size distribution with the maximum around 1.1 nm, but M3 and its monoliths have an important contribution of pores between 1.8 and 3 nm.

In summary, Fig. 1 and 3 allow us to see the different adsorption capacities of the two types of monoliths used and Fig. 2 and 4 their different pore size distributions; the A-series has lower, narrower and more homogeneous porosity than the high porosity monoliths (M3M and K1M).

The above results show that we have two types of selected monoliths; one having moderate porosity and high density and another having high porosity and moderate density, which will be very suitable for analyzing the importance of the way of expressing gas storage at room temperature (gravimetric/volumetric).

3.2. Gas storage at room temperature

To understand the importance that the textural properties (apparent BET surface area, micropore volume and pore size distribution) and the monolith densities have on the adsorption capacity on both a gravimetric and volumetric basis at room temperature, three different gases were selected as adsorbates: hydrogen, methane and carbon dioxide.

3.2.1. H_2 storage (RT and pressure < 200 bar). The gravimetric H_2 excess (wt%, *i.e.*, (g of H_2/(g of C + g of H_2) × 100)) adsorption isotherms of all the monoliths studied are shown in Fig. 5. The pristine carbon monoliths A1 and A3 already adsorb over 0.6 wt%, due to their remarkable narrow microporosity development (V_{DR} (CO_2): 0.44 and 0.45 $cm^3\ g^{-1}$, respectively). After activation with CO_2, their gravimetric adsorption amounts increase significantly, reaching values around 1 wt% for samples A3-12 and A3-48, corresponding to a V_{DR} (CO_2) of 0.5 $cm^3\ g^{-1}$. Samples M3M and K1M, which present the highest porosity development and narrow microporosity (around 0.6 $cm^3\ g^{-1}$), have the highest H_2 adsorption capacity on a gravimetric basis (over 1.1 wt%).

H_2 adsorption capacity of adsorbent materials on a gravimetric basis has been widely correlated with their porosity. When correlating the H_2 excess adsorption at 25 °C and up to 200 bar with the narrow microporosity (pore size < 0.7 nm, V_{DR} (CO_2)), a well defined trend can be found.[35] The results of Fig. 5 confirm the linear relation between the narrow micropore volume and the

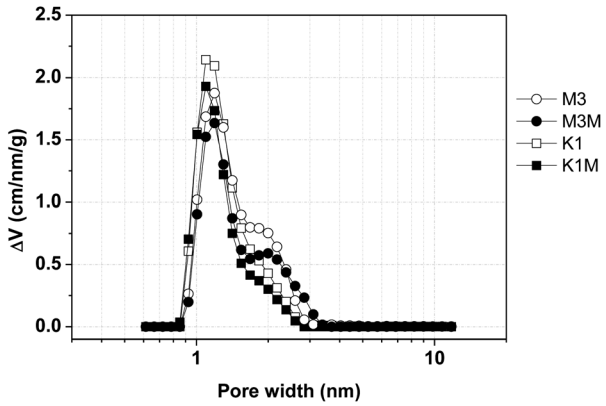

Fig. 4 DFT pore size distributions of the samples (M3 and K1) and their monoliths (M3M and K1M).

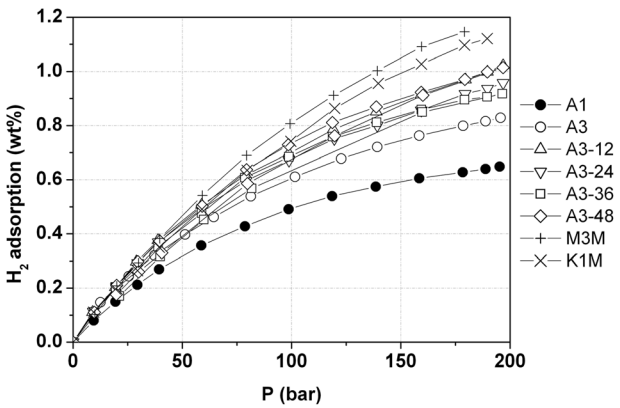

Fig. 5 H_2 excess adsorption isotherms at 25 °C on a gravimetric basis.

H_2 adsorption capacity on a gravimetric basis. The monoliths prepared from the granular activated carbons with well developed porosity show a higher H_2 uptake per gram of adsorbent than the activated samples derived from A-series monoliths. In summary, at room temperature and up to 200 bar, the higher the sample porosity (especially the narrow micropore volume) the higher will be the gravimetric H_2 adsorption. These observations confirm previous findings of a linear relationship between V_{DR} (CO_2) and gravimetric H_2 adsorption.[35]

When the adsorption capacity is expressed per litre of the sample, the above conclusion is no longer valid. In addition to the sample porosity, the density considerably affects the storage results. Thus, Fig. 6, which presents the H_2 excess adsorption isotherms on a volumetric basis, shows important differences from those of the gravimetric results of Fig. 5. The different sequences of the isotherms of both figures reveal a higher H_2 uptake by materials obtained from the A series when compared with the M3M and K1M monoliths, even for the unactivated A1 and A3 monoliths. Therefore, from the volumetric capacity results it can be observed that the higher piece density of the A series monoliths results in a higher H_2 uptake. Thus, more than 10 g l^{-1} are reached by the A3-12 sample, whereas the monoliths prepared from activated carbons with high porosity development reach less than 6 g l^{-1}. These values highlight the importance of the adsorbent density when the results are expressed in volumetric terms and are among the best published ones at room temperature and up to 200 bar for H_2 storage, as will be commented later on.

3.2.2. CH_4 storage (RT and pressure < 30 bar). In the case of methane storage, it is well known that its adsorption on porous materials at room temperature and high pressures takes place in micropores with a pore size around 1.1 nm.[36–39] This dependence on the micropore size distribution implies that the total micropore volume (V_{DR} (N_2)) is used to provide an indication of the adsorption capacity of the selected carbon monoliths. In this sense, and taking into account the characterization results of the selected samples (see Tables 1 and 2), it would be expected that, in the particular case of CH_4 adsorption, less differences among the monoliths would be obtained than for hydrogen gas. This is so because, while samples M3M and K1M show high total micropore volumes, the A series has narrow pore size distributions (see Fig. 2 and 4).

Fig. 7 presents the methane excess adsorption isotherms on a gravimetric basis (wt%, *i.e.*, g of CH_4/(g of C + g of CH_4) × 100) for each carbon monolith. It can be observed that, for the A series, the adsorption increases with the activation time. Thus, the highest CH_4 adsorption capacities correspond to the A3-48 sample, as well as the M3M which has the highest total micropore volume.

As was mentioned above, from an application point of view, the amount of gas that can be adsorbed per unit volume is a very important factor. Fig. 8 shows the CH_4 adsorption capacity calculated on a volumetric basis using the piece density of each sample. In this case, it can be observed that the A series monoliths present higher CH_4 uptake per litre of adsorbent, not only due to their higher density, but also due to their appropriate narrow micropore size distributions that also affect the CH_4 capacity. Values achieved on a gravimetric basis for our monoliths (12 wt%) are similar to those reported by Yeon *et al.* for CDC plates.[21] Thus, CDC plates adsorb about 13 wt% of CH_4 at 30 bar. Thanks to their higher density (1 g cm^{-3}) these samples achieve around 180 V/V at 30 bar, which is higher than that in our case (110 g l^{-1}, which corresponds to 154 V/V). These high values point out the importance of the material density for achieving high adsorption capacities.

3.2.3. CO_2 storage (RT and pressure < 30 bar). Due to the environmental impact of carbon dioxide, an important application is its capture and transport. The results obtained at room temperature and up to 30 bar are plotted in Fig. 9 (on a gravimetric basis; *i.e.*, g of CO_2/(g of C + g of CO_2) × 100) and in Fig. 10 (on a volumetric basis).

An analysis of the influence that the sample properties have on the gravimetric results indicates that, when the pressure is in the range of 1 and 10 bar, the amount of CO_2 adsorbed at 25 °C is controlled by the narrow micropore volume.[18] However, for pressures higher than 10 bar, the total micropore volume (or apparent BET surface area) controls the uptake. Thus, these parameters are good indicators for knowing the behaviours of different samples with regard to CO_2 storage at 30 bar and room temperature. These observations indicate that the storage of CO_2 at room temperature is sensitive to both, the pore size distribution and the storage pressure used. As was expected, according to the textural characterization, M3M and K1M (2610 and 2320 m^2 g^{-1}, respectively) show a significantly higher CO_2 uptake than

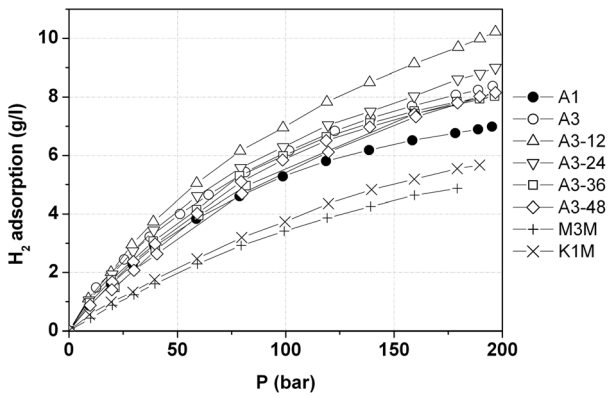

Fig. 6 H_2 excess adsorption isotherms at 25 °C on a volumetric basis.

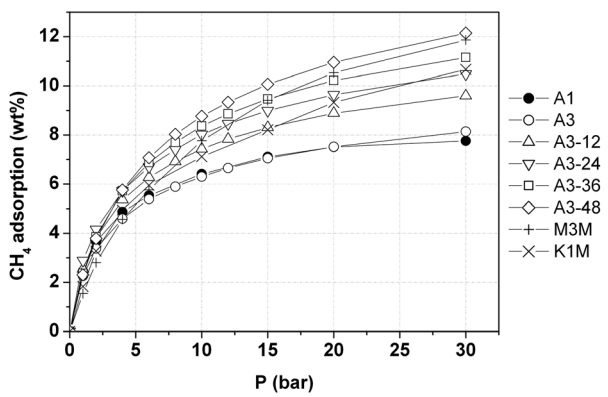

Fig. 7 CH_4 excess adsorption isotherms at 25 °C on a gravimetric basis.

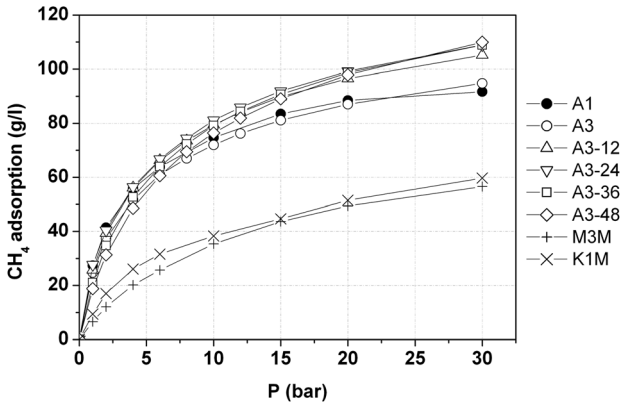

Fig. 8 CH_4 excess adsorption isotherms at 25 °C on a volumetric basis.

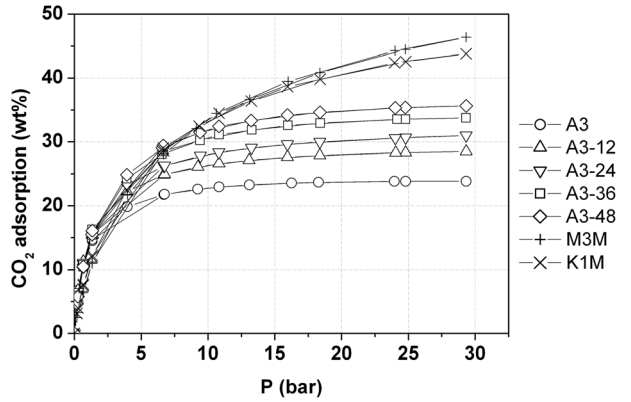

Fig. 9 CO_2 excess adsorption isotherms at 25 °C on a gravimetric basis.

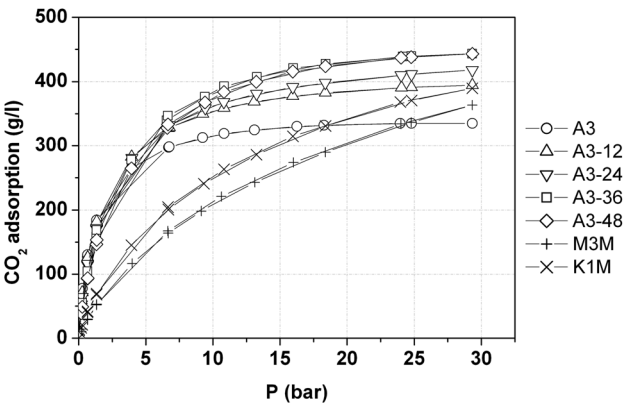

Fig. 10 CO_2 excess adsorption isotherms at 25 °C on a volumetric basis.

monoliths from the A series, around two times higher compared with the original sample (A3). On the other hand, the increase in the activation time provokes a higher porosity development (Table 1) and, subsequently, an increase in the CO_2 uptake, reducing the differences among M3M and K1M and the monoliths of the A series.

When the CO_2 adsorption capacity is expressed per litre of adsorbent instead of per gram of adsorbent, the obtained trends are completely different. CO_2 adsorption isotherms on a volumetric basis are shown in Fig. 10. It can be observed that all the selected monoliths show more or less similar adsorption capacities at the highest pressure used (30 bar). However, CO_2-activated monoliths present an adsorption capacity slightly higher than those for samples M3M and K1M, reaching more than 400 gCO_2/l. Once again, the comparison of the results obtained from the A series samples (high densities and moderate porosities) and from the monoliths M3M and K1M (high adsorption capacities and moderate densities) allows a demonstration of the important role of the density on the volumetric capacity.

3.2.3.1. Scale-up study for RT CO_2 storage in an A1 sample. Most experiments in articles deal with the data measured only by sorption equipments using a small amount of samples and hence it is hard to find reference data for evaluating the performance of certain materials under practical conditions. This scale-up study at RT for carbon dioxide storage can be considered a further complementary step.

Based on the CO_2 storage data presented above, an additional analysis for CO_2 storage will be discussed next using a much higher scale, for the commercial A1 sample. First, we present Fig. 11 to compare the CO_2 isotherms for two monoliths studied before: the commercial A1 and the monolith prepared from Maxsorb3000 (M3M). Fig. 11a shows the excess adsorption on a gravimetric basis and Fig. 11b their total storage capacities on a volumetric basis. Here we introduce for the first time in this work the total storage capacity parameter, which corresponds to the total amount of gas that can be loaded in a tank filled with an

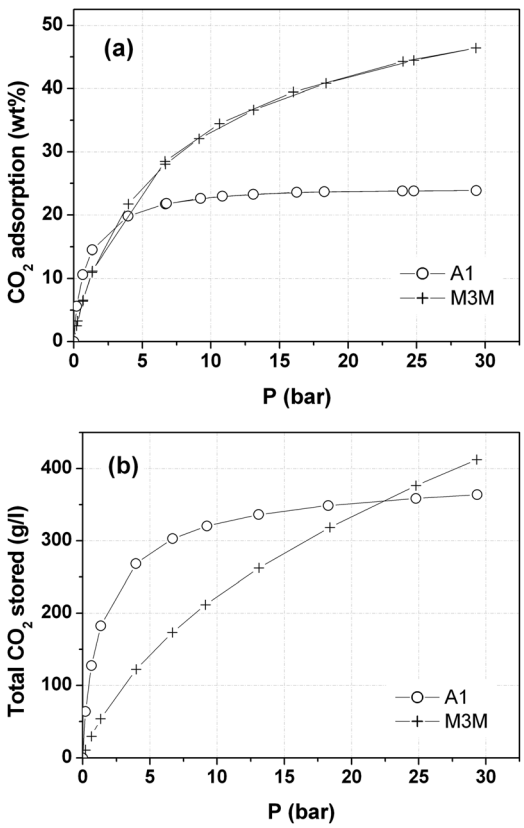

Fig. 11 (a) CO_2 excess adsorption isotherms at 25 °C on a gravimetric basis for A1 and M3M carbon monoliths and (b) their total CO_2 storage capacity.

adsorbent and it includes the excess adsorbed gas and the gas compressed in the space not occupied by atoms of the material. This parameter can be obtaining from the excess adsorption isotherm by applying a simple equation.[1,3,8,20] Therefore, the values reported in Fig. 11b (corresponding to laboratory scale) can be compared with ones obtain in the scale-up study (see Table 3).

As discussed above, the conclusion about the adsorption capacity of a sample that can be obtained from these figures depends very much on the way used to express the results (on wt% basis – *i.e.*, gravimetric basis – or on a volumetric basis). In Fig. 11a it can be seen that M3M has a higher performance presenting much higher uptake than the A1 carbon monolith. Contrarily, the differences between their total storage capacities (Fig. 11b) are reduced drastically, being quite similar for both samples or better for sample A1, depending on the pressure used. In fact, for pressures lower than 20 bar, A1 reaches higher CO_2 storage capacities than the M3M monolith. This is due to the fact that A1 has higher density than the M3M monolith and therefore a higher amount of the A1 sample can be put inside a tank.

The scaled-up CO_2 storage was studied for the carbon monoliths, using two tanks with the same volume (2.5 l): one remaining empty and the other one being filled with 2.64 kg of A1 carbon monoliths (see picture of Fig. 12).

CO_2 storage measurements were carried out up to 20 bar and at 20 °C, a temperature and a pressure somewhat lower than those in the case of the adsorption isotherms. The amount of CO_2 stored was obtained by the increment of weight before and after storage (see Fig. 12, right). Table 3 presents the data obtained from the activated carbon-filled and empty cylinders.

Two points of merit are noticed: (i) laboratory and scale-up results are very close to confirming the suitability of the results obtained (both gravimetric and volumetric) and (ii) comparing the results obtained by adsorption on activated carbon per unit volume with the amount of CO_2 stored by compression, it can be clearly seen that the adsorption process has important advantages. Thus, the amount of CO_2 stored per unit volume in the tank that contains activated carbon is higher than the CO_2 stored by compression in the empty tank. For the studied pressure of 20 bar, the carbon-filled cylinder can store 376 g l^{-1}, while the amount stored by compression is only 40 g l^{-1}. Thus, nearly 10 times the amount of CO_2 can be stored by adsorption in comparison with simple compression, marking an important advantage among published results claiming the best CO_2 storage capacities.[1,11]

Table 3 Comparison of the CO_2 storage by compression and adsorption on A1 under practical conditions in a tank cylinder

Empty cylinder		Cylinder filled with A1	
Pressure (bar)	Weight (g)	Pressure (bar)	Weight (g)
0	4640	0	7280
20	4740	20	8220
Increment (g of CO_2)	100	Increment (g of CO_2)	940
Storage capacity			
Theoretical (25 °C)[a]	Real (20 °C)	Theoretical (25 °C)[a]	Real (20 °C)
39 g l^{-1}	40 g l^{-1}	350 g l^{-1}	376 g l^{-1}

[a] From results obtained at 25 °C.

Fig. 12 Pictures of the two cylinders used for the CO_2 scale up study (left), CO_2 pressurizing charging system (centre) and uptake measurement (right).

3.3. Importance of the adsorbent density for volumetric storage performances

Independent of the gas used (H_2, CH_4 or CO_2), the conclusions obtained from the performances of the different monoliths studied when they are expressed on a gravimetric basis (Fig. 5, 7 and 9) completely differ from those when the results are expressed on a volumetric basis (Fig. 6, 8 and 10). In general, and for the three gases studied, one can observe that for adsorption on a gravimetric basis, the textural properties are very important, since the adsorbents with increased development of porosity reach higher values. However, on a volumetric basis, the density of the adsorbent material plays a key role. Thanks to their high density, carbon monoliths exhibit an adsorption per litre of sample that exceeds values obtained for samples with much higher developed porosity. As discussed above, such observations confirm that the density of the material has the most important impact on a gas storage capacity, particularly useful for vehicle and/or transport applications. This observation, not restricted to the samples analysed in this work, can be well summarized in the following, where we compare the obtained results with those from the literature.

3.3.1. Comparison with other carbon sorbents. Fig. 13 compiles, for the three gases studied, the volumetric adsorption capacities, plotted over the porosity of the adsorbent. In the case of H_2, the narrow micropore volume (V_{DR} (CO_2) is used, while the CH_4 and CO_2 adsorption capacities are represented over the total micropore volumes (V_{DR} (N_2)). The results obtained for the A series monoliths are represented by filled circles and for the K1M and M3M monoliths as empty squares. For comparison, results of other activated carbon materials are also shown (filled triangles).[35,36] It can be observed that, for all of the investigated gases, the higher densities of the A series monoliths cause them to reach the highest volumetric adsorption capacities, even in comparison with samples which have much more developed porosities. This emphasizes the importance of the adsorbent density for gas storage at room temperature and the suitability of the A series monoliths for this kind of application. It has to be highlighted that the activated carbon materials from the literature are powdered samples, and that their packing densities were used for calculating their volumetric capacities.[35,36] Therefore

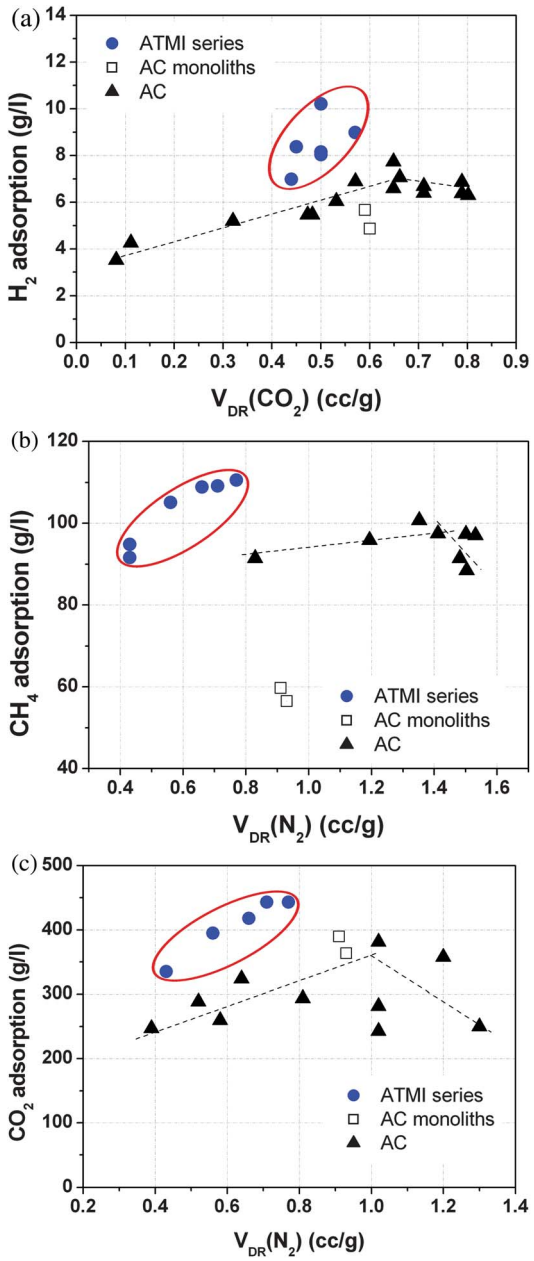

Fig. 13 Volumetric adsorption capacities obtained at 25 °C over porosity. (a) H_2 over V_{DR} (CO_2),[35] (b) CH_4 over V_{DR} (N_2),[36] and (c) CO_2 over V_{DR} (N_2).

they need a mechanical pressure for compacting. The use of such pressure is an additional drawback in comparison with the piece density of the monolith materials which, additionally, can be handled more easily than compacted powder activated carbons. In general, our findings agree with those from the literature where adsorption on carbon monoliths was measured. Thus, there are a few carbon specialists who have focused their efforts on achieving high volumetric capacities by preparing monoliths and pieces with high density[3,20,21,40] and in certain cases, they have demonstrated ways to produce small quantities of such materials. Nevertheless, we feel that the outstanding volumetric results reported here signify what is achievable because these monoliths are commercially available.

3.3.2. Comparison with one of the most outstanding sorbents (MOF-210). To confirm the relative importance that the sample surface area might have, in relation to its density, in its volumetric storage capacity, we compare the adsorption performance of some of our monoliths (A1, A3-36, and M3M) with results obtained using the same gases and the same experimental conditions on the material that exhibits the highest surface area (6240 m^2 g^{-1}) reported to date (MOF-210).[11,41,42]

Fig. 14 presents the gravimetric adsorption isotherms for H_2, CH_4 and CO_2 of the samples compared. In the case of all three gases it can be seen that with increasing pressures M3M and MOF-210 reach higher values in comparison with A1 and A3-36. This is due to their much large surface areas which provide more adsorption sites under these conditions.

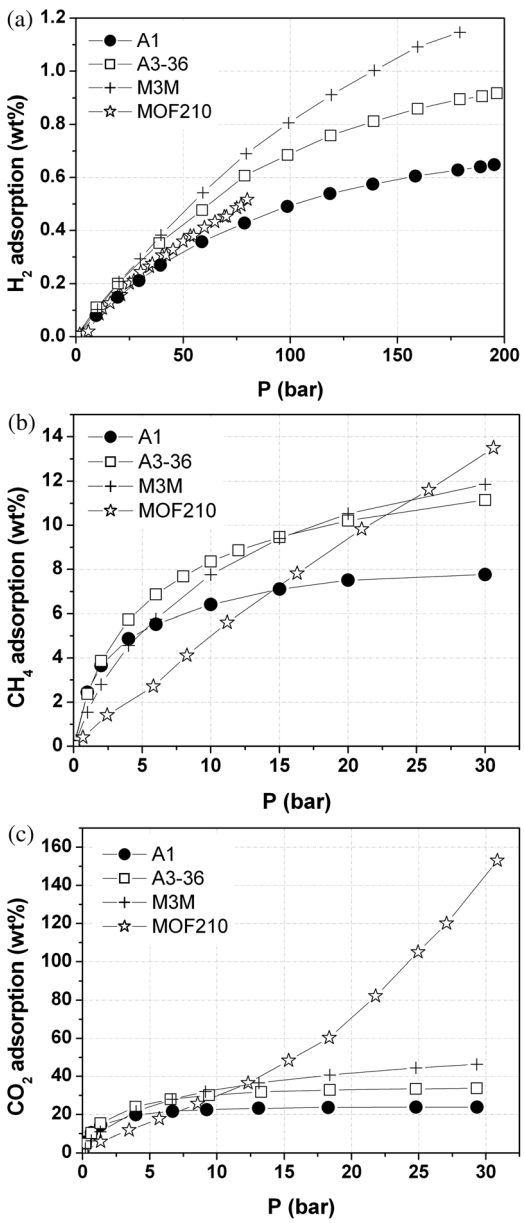

Fig. 14 Gravimetric adsorption isotherms of (a) H_2, (b) CH_4, and (c) CO_2 obtained at 25 °C for samples A1, A3-36, M3M and MOF-210.[11,41]

Fig. 15 presents the volumetric adsorption isotherms of these samples. In the case of the monolith samples, their piece densities were used to calculate their volumetric adsorption, whereas for MOF-210 its crystal density (0.25 g cm^{-3}) was used.[11] Even though the use of its crystal density will overestimate its volumetric uptake,[1,8,16] Fig. 15 reveals that, in general, MOF-210 reaches much lower volumetric adsorption amounts than the monoliths. For H_2 and CH_4 adsorption, the values of MOF-210 are lower throughout the pressure range measured. In the case of CO_2 adsorption, MOF-210 requires high pressures around 30 bar in order to reach similar values than the monoliths.

Although other MOFs (*e.g.*, MOF-5)[10] might outperform the volumetric uptake of MOF-210, due to its low crystal density, the comparison in terms of volumetric capacity between carbon materials and MOFs should be done with great caution. Most published MOF results claim outstanding gas storage performances in comparison with any other adsorbents. These claims are certainly true when the results are expressed on a gravimetric basis but not on a volumetric basis if their crystal densities are used to convert their gravimetric data to volumetric ones. An example of what is currently accepted can be seen in the paper by J. Sculley *et al.*[43] where the best MOFs for hydrogen storage (more than 200) are listed and their volumetric capacities are calculated using crystal densities. Under these conditions these volumetric capacities are overestimated, assuming that the tank is filled with a monocrystal of MOF, as has been deeply analyzed in some works.[1,3,8,16,20,44]

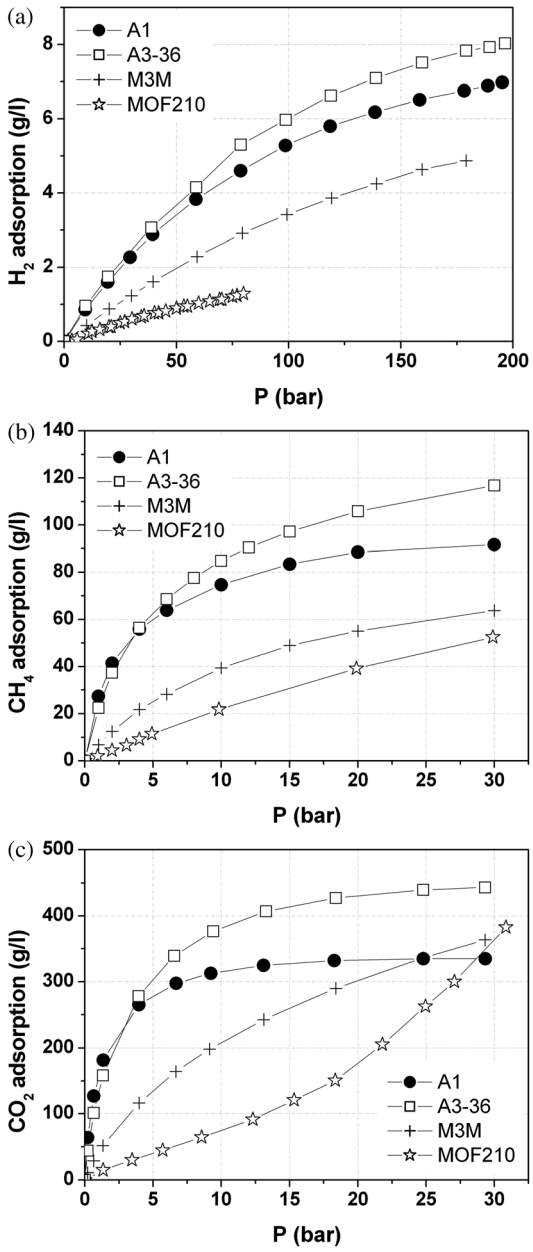

Fig. 15 Volumetric adsorption isotherms of (a) H_2, (b) CH_4, and (c) CO_2 obtained at 25 °C for samples A1, A3-36, M3M and MOF-210.[11,41] In the case of MOF-210, the published crystal density (0.25 g cm^{-3})[11] was used to obtain the volumetric uptake.

In summary, the volumetric adsorption results for H_2, CH_4 and CO_2 at RT obtained with ATMI monoliths and the CO_2-activated carbon monoliths obtained from them are, to the best of our knowledge, higher than those for any other adsorbents reported in the literature.[1,11,41]

4. Conclusions

From the high pressure adsorption isotherms (H_2, CH_4 and CO_2) measured at room temperature on two types of adsorbent monoliths, one with high density values but moderate porosities (A series) and the other one with moderate densities and high porosity developments (M3M and K1M), the following conclusions can be drawn:

(1) Independent of the adsorbent nature, the gas storage takes place by a physisorption process, which is controlled by the properties of the adsorbent material (porosity and density) and also by the nature of the adsorbate.

(2) For a given gas, the storage capacities of the adsorbents depend on: (i) their textural properties, when the results are expressed on a gravimetric basis and (ii) their textural properties and densities when the results are expressed on a volumetric basis, the density having the most important impact on gas storage capacity, useful for vehicle and/or transport applications.

(3) Due to their singular high density, the ATMI monolith, as well as its CO_2 activated monoliths, present exceptionally high volumetric storage capacity for H_2, CH_4 and CO_2 at room temperature.

(4) Exceptionally high volumetric storage capacities have been obtained using piece densities of the monoliths which, to the best of our knowledge, are amongst the highest that have been reported; higher than the high surface area samples M3M monolith prepared from Maxsorb (S_{BET}: 2610 m^2 g^{-1}) or MOF-210 (S_{BET}: 6240 m^2 g^{-1}).

Acknowledgements

The authors thank the Generalitat Valenciana and FEDER (project PROMETEO/2009/047) for financial support.

References

1 A. Linares-Solano, D. Cazorla-Amorós, J. P. Marco-Lozar and F. Suárez-García, in *Coordination Polymers and Metal Organic Frameworks*, ed. O. L. Ortiz and L. D. Ramírez, Nova Science Publishers Inc., New York, 2011, pp. 197–224.

2 J. Yang, A. Sudik, C. Wolverton and D. J. Siegel, *Chem. Soc. Rev.*, 2010, **39**, 656.
3 A. Linares-Solano, M. Jordá-Beneyto, M. Kunowsky, D. Lozano-Castelló, F. Suarez-Garcia and D. Cazorla-Amorós, in *Carbon Materials: Theory and Practice*, ed. A. P. Terzyk, P. A. Gauden and P. Kowalczyk, Research Signpost, Kerala, 2008, pp. 245–281.
4 P. Benard and R. Chahine, *Scr. Mater.*, 2007, **56**, 803.
5 M. G. Nijkamp, J. E. M. J. Raaymakers, A. J. van Dillen and K. P. de Jong, *Appl. Phys. A: Mater. Sci. Process.*, 2001, **72**, 619.
6 A. W. C. van den Berg and C. O. Arean, *Chem. Commun.*, 2008, 668.
7 K. M. Thomas, *Dalton Trans.*, 2009, **9**, 1487.
8 J. P. Marco-Lozar, J. Juan-Juan, F. Suárez-García, D. Cazorla-Amorós and A. Linares-Solano, *Int. J. Hydrogen Energy*, 2012, **37**, 2370.
9 J. E. Lennard-Jones, *Trans. Faraday Soc.*, 1932, **28**, 333.
10 H. Furukawa and O. M. Yaghi, *J. Am. Chem. Soc.*, 2009, **131**, 8875.
11 H. Furukawa, N. Ko, Y. B. Go, N. Aratani, S. B. Choi, E. Choi, A. O. Yazaydin, R. Q. Snurr, M. O'Keeffe, J. Kim and O. M. Yaghi, *Science*, 2010, **329**, 424.
12 M. Eddaoudi, J. Kim, N. Rosi, D. Vodak, J. Wachter, M. O'Keeffe and O. M. Yaghi, *Science*, 2002, **295**, 469.
13 T. Kyotani, T. Nagai, S. Inoue and A. Tomita, *Chem. Mater.*, 1997, **9**, 609.
14 Z. Ma, T. Kyotani and A. Tomita, *Carbon*, 2002, **40**, 2367.
15 D. Zhao, D. J. Timmons, D. Yuan and H. C. Zhou, *Acc. Chem. Res.*, 2010, **44**, 123.
16 J. Juan-Juan, J. P. Marco-Lozar, F. Suarez-Garcia, D. Cazorla-Amorós and A. Linares-Solano, *Carbon*, 2010, **48**, 2906.
17 S. J. Yang, J. H. Im, H. Nishihara, H. Jung, K. Lee, T. Kyotani and C. R. Park, *J. Phys. Chem. C*, 2012, **116**, 10529–10540.
18 V. Presser, J. McDonough, S.-H. Yeon and Y. Gogotsi, *Energy Environ. Sci.*, 2011, **4**, 3059–3066.
19 M. Jordá-Beneyto, F. Suarez-Garcia, D. Lozano-Castelló, D. Cazorla-Amorós and A. Linares-Solano, *Carbon*, 2007, **45**, 293–303.
20 M. Jordá-Beneyto, D. Lozano-Castelló, F. Suarez-Garcia, D. Cazorla-Amorós and A. Linares-Solano, *Microporous Mesoporous Mater.*, 2008, **112**, 235–242.
21 S.-H. Yeon, I. Knoke, Y. Gogotsi and J. E. Fischer, *Microporous Mesoporous Mater.*, 2010, **131**, 423–428.
22 R. Zacharia, D. Cossement, L. Lafi and R. Chahine, *J. Mater. Chem.*, 2010, **20**, 2145–2151.
23 R. Chahine and T. K. Bose, *Int. J. Hydrogen Energy*, 1994, **19**, 161.
24 M. Kunowsky, J. P. Marco-Lozar, A. Oya and A. Linares-Solano, *Carbon*, 2012, **50**, 1407.
25 H. Reardon, J. M. Hanlon, R. W. Hughes, A. Godula-Jopek, T. K. Mandal and D. H. Gregory, *Energy Environ. Sci.*, 2012, **5**, 5951–5979.
26 D. Lozano-Castelló, M. A. Lillo-Ródenas, D. Cazorla-Amorós and A. Linares-Solano, *Carbon*, 2001, **39**, 741.
27 D. Lozano-Castello, D. Cazorla-Amoros, A. Linares-Solano and D. F. Quinn, *Carbon*, 2002, **40**, 2817.
28 F. Rodriguez-Reinoso and A. Linares-Solano, *Chem. Phys. Carbon*, 1988, **21**, 1.
29 D. Cazorla-Amoros, J. Alcañiz-Monge and A. Linares-Solano, *Langmuir*, 1996, **12**, 2820.
30 D. Cazorla-Amoros, J. Alcañiz-Monge, M. A. de la Casa-Lillo and A. Linares-Solano, *Langmuir*, 1998, **14**, 4589.
31 E. Gadea-Ramos, F. Suarez-Garcia, D. Cazorla-Amorós, M. Jordá-Beneyto and A. Linares-Solano, Patent WO2008107505–A1, 2008.
32 B. A. Younglove, *J. Phys. Chem. Ref. Data*, 1982, **11**, 1.
33 R. K. Agarwal and J. A. Schwarz, *Carbon*, 1988, **26**, 873.
34 J. P. Singer, A. Mayergoyz, C. Portet, E. Schneider, Y. Gogotsi and J. E. Fischer, *Microporous Mesoporous Mater.*, 2008, **116**, 469–472.
35 M. Kunowsky, J. P. Marco-Lozar, D. Cazorla-Amorós and A. Linares-Solano, *Int. J. Hydrogen Energy*, 2010, **35**, 2393.
36 D. Lozano-Castello, J. Alcañiz-Monge, M. A. de la Casa-Lillo, D. Cazorla-Amorós and A. Linares-Solano, *Fuel*, 2002, **81**, 1777.
37 J. Alcañiz-Monge, D. Lozano-Castello, D. Cazorla-Amorós and A. Linares-Solano, *Microporous Mesoporous Mater.*, 2009, **124**, 110.
38 D. Lozano-Castello, D. Cazorla-Amorós, A. Linares-Solano and D. F. Quinn, *Carbon*, 2002, **40**, 989.
39 A. Celzard and V. Fierro, *Energy Fuels*, 2005, **19**, 573–583.
40 C. Vakifahmetoglu, V. Presser, S.-H. Yeon, P. Colombo and Y. Gogotsi, *Microporous Mesoporous Mater.*, 2011, **144**, 105–112.
41 O. M. Yaghi, *DOE Hydrogen Program*, 2011.
42 H. Reardon, J. M. Hanlon, R. W. Hughes, A. Godula-Jopek, T. K. Mandal and D. H. Gregory, *Energy Environ. Sci.*, 2012, **5**, 5951–5979.
43 J. Sculley, D. Yuan and H.-C. Zhou, *Energy Environ. Sci.*, 2011, **4**, 2721–2735.
44 J. Donald Carruthers, M. A. Petruska, E. A. Sturm and S. M. Wilson, *Microporous Mesoporous Mater.*, 2012, **154**, 62–67.

